

Mineralization mechanisms of groundwater in a semi-arid area in Algeria: statistical and hydrogeochemical approaches

F. Bouteldjaoui, M. Bessenasse, J.-D. Taupin and A. Kettab

ABSTRACT

The study area of Ain Oussera (3,790 km²) is located in the semi-arid high plains of the Saharian Atlas (200 km south of Algiers). Groundwater investigated in the present study is from the Albian formations which are considered as a major source for drinking and irrigation water. The objective of this study is to identify the different hydrochemical processes controlling the groundwater mineralization. For this purpose, chemical analyses were performed on 31 wells sampled during May 2014. The chemical study (total dissolved solids (TDS), Piper, chemical correlation) allowed the origins of groundwater mineralization to be identified. The dissolution of evaporate minerals, precipitation of carbonate minerals, and ion exchange reactions have been identified as major sources of mineralization processes. Anthropogenic processes due to human activities (sewage effluents and agricultural fertilizers) also contribute to the mineralization of the water. The results of principal component analysis also confirm that both natural and anthropogenic processes contribute to the chemical composition of groundwater in the study area.

Key words | Algeria, hydrogeochemistry, multivariate statistical analysis, semi-arid zone, water quality

F. Bouteldjaoui (corresponding author)

A. Kettab

Laboratoire de Recherche Sciences de l'Eau
(LRS-EAU/ENP),
Ecole Nationale Polytechnique (ENP),
10, Av. HacénBadi, BP 182, El-Harrach-Alger,
Algeria
E-mail: theldjaoui@yahoo.fr

M. Bessenasse

Université Saad Dahlab,
Soumaa, 09000 Blida,
Algeria

J.-D. Taupin

Laboratoire HydroSciences (IRD, CNRS, UMI),
300 Avenue du Professeur Emile Jeanbrau,
Montpellier,
France

INTRODUCTION

Groundwater chemistry is largely determined by natural processes (aquifer lithology, flow direction, water–rock/soil interactions in the unsaturated and saturated zones, and residence time), and anthropogenic activities (agriculture, industry, urban development, and overexploitation of groundwater resources) (Li *et al.* 2017). Understanding the principal processes that control groundwater chemistry is important for sustainable development and effective management of groundwater resources in any area (Wu *et al.* 2017). The plain of Ain Oussera, located in the central part of northern Algeria, is characterized by a semi-arid climate (Kettab *et al.* 2008). Groundwater is a significant source for drinking water supply and irrigation of agricultural land in many parts of this area. Continuously increasing abstraction of groundwater resources to meet

rising agricultural and domestic needs leads to a growing deficit of water. However, intensive exploitation of the available water resources, coupled with periods of drought, have led to lowering of the water table and the increased risk of degradation of water quality, especially when abstraction amounts greatly exceed the natural recharge of aquifers. As a multivariate analysis method, principal component analysis (PCA) has been successfully applied to distinguish natural and anthropogenic sources affecting groundwater chemistry (Cloutier *et al.* 2008). In the study of Farnham *et al.* (2003), the application of multivariate statistical analysis to trace element chemistry of groundwater helped identify rock–water interaction processes and groundwater redox conditions. The combined use of statistical methods and hydrochemical

analysis constitutes effective approaches that help in the interpretation of hydrochemical data and identification of possible factors/sources that influence water geochemistry (Cloutier *et al.* 2008; Wu *et al.* 2014, 2019; Li *et al.* 2019).

The aim of this study is to identify the main factors and mechanisms controlling the chemistry in the Ain Oussera plain, using geochemical and multivariate statistical methods such as PCA. This research will help current water resources planning in the area and provide some basic data for the rational exploitation and use of water resources in the future.

MATERIALS AND METHODS

Study area

The Ain Oussera plain (Figure 1(a)) is located in the central part of northern Algeria between longitudes 2°20' and 3°45' E and latitudes 34°55' and 35°40' N, and covers approximately an area of 3,790 km². The study area is bordered in the north by the Ain Oussera mountains (Koudiat el Gherbania, Koudiat el Taïcha, Koudiat el Mouilah and Kef Nesser), in the east by the Djebel Touil, and in the west by the Touil wadi (intermittent river). In the south, it is limited by the Sebaa Rous and Gueltet Essthel mountain range. The altitudes of the plain increase southwards, ranging between 700 and 800 m above mean sea level (amsl). The plain has a semi-arid climate type characterized by dry and hot summer and wet and cool winter seasons (Mebrouk 1994). The mean annual rainfall recorded at Ain Oussera meteorological station (from 1991 to 2011) is 231 mm, and the mean monthly temperature varies from 1.6 °C (January) to 37.7 °C (July). The rainfall season extends from October until March with the dry period between April and September. The annual mean potential evapotranspiration is 936.5 mm (1991–2011). Groundwater from the Albian sandstone aquifer (Lower Cretaceous) of Ain Oussera represents an important source for drinking water, agricultural and industrial purposes due to the scarcity of surface water (Maoui *et al.* 2013).

Geology and hydrogeology

The regional geology of the studied area has been investigated by several authors and forms a series of anticlines (Maoui *et al.* 2013). The region of Ain Oussera is a vast anticline with a Cretaceous axial part mainly oriented ENE–WSW (Figure 1(a) and 1(b)). The Plio-Quaternary and the Quaternary outcrops occupy a large part of the Ain Oussera plain, and are represented by actual and recent alluvial deposits: conglomerates, gravels, silts, crust, calcareous, etc. Miocene deposits are generally composed of sandstone, marls, and clays, as well as sandstone and limestone, and generally outcrop at the west of the plain with a thickness of approximately 170 m (Mebrouk 1994).

The axis of the principal anticline (ENE–WSW) passes by Jebel Touil to the east, Boucedria and Sidi Aissa to the west. This structure is complicated north and south by second-order structures. To the west of Ain Oussera, there is an anticline consisting of Koudiat Doghmane and Khatoua whose formations belong to the Lower Cretaceous. In the east part (Birine region), the Eocene terrains are affected by a scale structure, with secondary disturbance. From Guelt Es Stel to Bouira Sahary, the main structure is represented by the anticline of Khreidzer, framed by oblique faults. To the west, and to Taguine, extends a monoclin (cuesta) which constitutes the southern flank of the broad anticlinal zone, extending up to the Ain Oussera mountain range. In the north-west of the plain, one also observes Baremo-Aterévian anticlinal, crossed by a fault ENE–WSW. In general, folds and accidents are oriented approximately in an Atlas direction N 55° E to N 60° E (Maoui *et al.* 2013).

From a hydrogeological point of view, the Albian sandstone formations constitute the most extensive aquifer in the Saharian Atlas band (Intercalary Continental aquifer). The average thickness of the Albian sandstone aquifer is about 200 m in the major part of the plain (Mebrouk 1994). The Albian sandstone is the greatest aquifer in the region. It outcrops in several areas, mainly in the center of the plain where the water table is unconfined (Mebrouk *et al.* 2007). Elsewhere, the aquifer may be confined or semi-confined. The Albian substratum consists of limestones and sandstones, with marly levels of the Aptian age. Pumping tests indicate that the

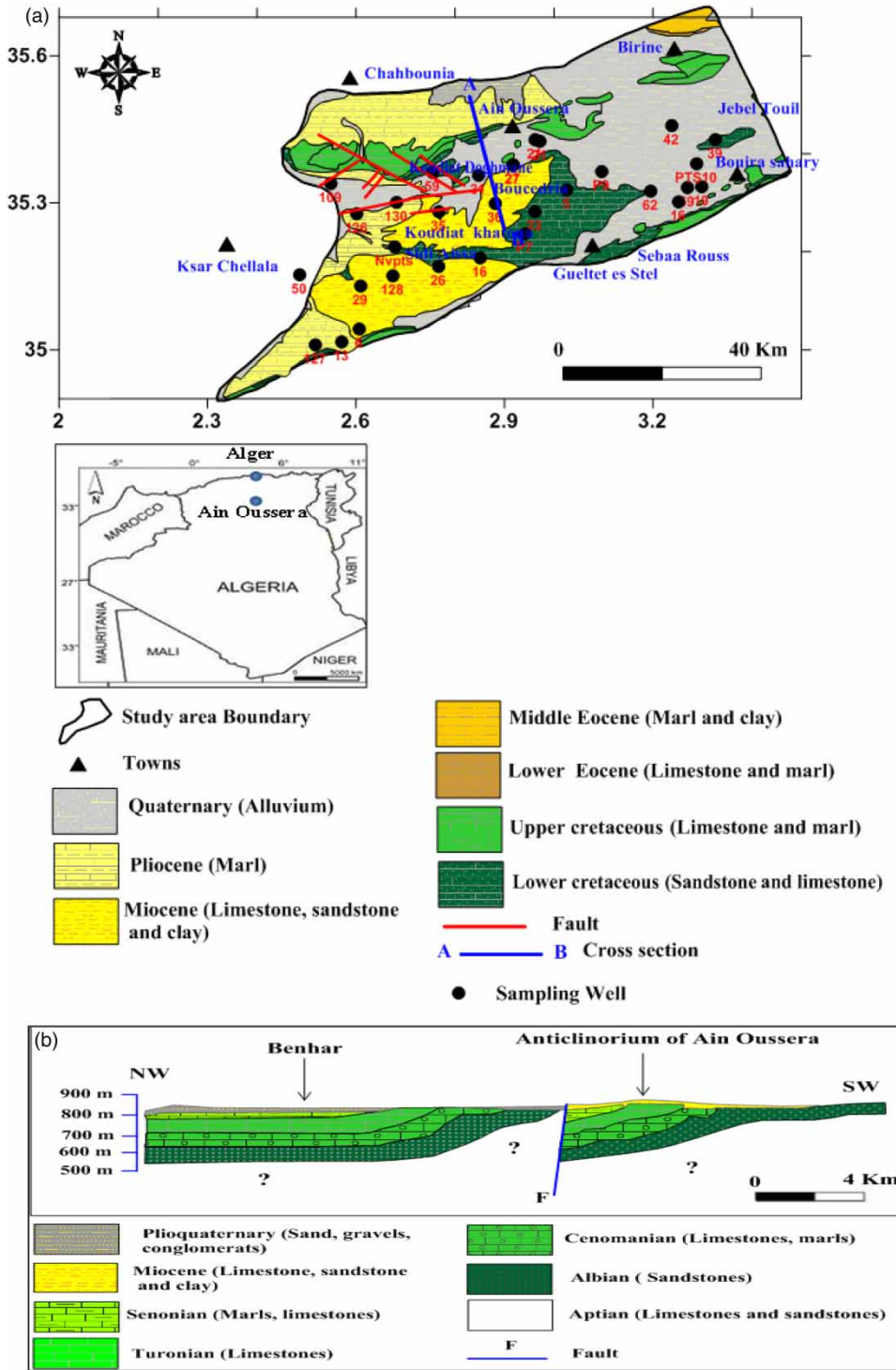


Figure 1 | (a) Geological map of the study area and groundwater sample locations. (b) Synthetic geological cross section, along transect (AB) (Maoui et al. 2013).

transmissivity in the upper part of the aquifer varies between 10^{-3} and $10^{-5} \text{ m}^2 \cdot \text{s}^{-1}$, and hydraulic conductivity ranges from 10^{-2} to 10^{-6} ms^{-1} . The groundwater flow is

generally towards the north, and the sandstone aquifer receives a direct alimentation from the southern limit (Cretaceous formation of Guelt-stel and Sebaa Rouss).

Sampling and analytical methods

A sampling campaign was performed during May 2014 with 31 groundwater samples (Figure 1(a)) being collected from the Albian aquifer. Measurements, including temperature, pH, alkalinity (HCO_3^-), electrical conductivity (EC), and total dissolved solids (TDS) were carried out in the field, using portable Orion EC and pH meters after recalibration with standard buffer solutions. Water samples were filtered through a $0.45\ \mu\text{m}$ cellulose membrane and collected in 100 mL polyethylene bottles in two sets. One was acidified with ultrapure acid (HNO_3) to $\text{pH} < 2$ for the determination of cations while the other was collected without adding any preservatives to determine the presence of anions. Chemical analyses of water samples were carried out in the Laboratory of the National Agency for Water Resources (ANRH) in Algeria. Cations (Ca^{2+} , Mg^{2+} , Na^+ , K^+) were analyzed by atomic absorption spectrometry, anions (Cl^- , SO_4^{2-} , and NO_3^-) by high performance ionic liquid chromatography (HPILC). Bicarbonates (HCO_3^-) were determined by acid–base titration method. The obtained results were tested for accuracy by calculating the ionic balance errors. The analytical precision of the ionic balance for all samples is within $\pm 5\%$ (Domenico & Schwartz 1998).

Multivariate statistical analysis

Multivariate statistical analyses including hierarchical cluster (HCA) and PCA has been established as a powerful tool for analyzing the complex high dimensional hydrochemical data sets of groundwater and identifying major natural and anthropogenic processes governing groundwater geochemistry (Cloutier *et al.* 2008; Wu *et al.* 2014, 2019; Li *et al.* 2019). PCA is a multivariate statistical technique widely used for data reduction in hydrochemical and hydrogeological studies (Farnham *et al.* 2003). In addition, it reduces the dimensionality of the chemical data set with correlated variables by creating new uncorrelated variables (the PCs) that are a linear combination of the original data linear combination of the original data (Voutsis *et al.* 2015). An important step in PCA is to determine the optimum number of components to retain. In this study, the Kaiser criterion (Kaiser 1958) was applied to determine the total number of factors that could summarize

the data set. Under this criterion, only factors with eigenvalues greater than or equal to 1 will be considered as possible sources of variance in the data. The obtained factors are classified in such a way that the first principal component has the highest eigenvalue and represents the most sources of variation of the original data (Everitt & Hothorn 2011). The factor loadings are interpreted as correlation coefficient between the variable and principal components. In this study, PCA was applied to chemical data to analyze the principal factors corresponding to the different processes that control water chemistry and sources of variation in the data.

Saturation index

The saturation index (SI) of a mineral is useful to understand the different stages of hydro-geochemical evolution and it helps in identifying geochemical processes responsible for chemical characteristics of groundwater. The values of SIs indicate the tendency of minerals to dissolve or precipitate in the groundwater aquifer system. In this study, SI was calculated using the PHREEQC program (Parkhurst & Appelo 2011) based on the following equation:

$$SI = \log(IAP/K_{sp}) \quad (1)$$

where IAP is the ion activity product and K is the equilibrium constant. Equilibrium is indicated when $SI = 0$; the groundwater is oversaturated with respect to the particular mineral when $SI > 0$, which means that the mineral phase may precipitate to achieve equilibrium. If $SI < 0$, the groundwater is undersaturated with mineral phase, which means that dissolution is required to reach equilibrium (Zaidi *et al.* 2016).

RESULTS AND DISCUSSION

A statistical summary of groundwater hydrochemical parameters is presented in Table 1. The pH values ranged from 7.1 to 8.8, indicating neutral to slightly alkaline water. The total dissolved solids and the EC values range from 468 to 2,741 mg/L and 650 to 5,150 $\mu\text{S}/\text{cm}$, with average values of 1,150.5 mg/L and 1,929.4 $\mu\text{S}/\text{cm}$. According to

Table 1 | Statistical summary of physico-chemical parameters in the study

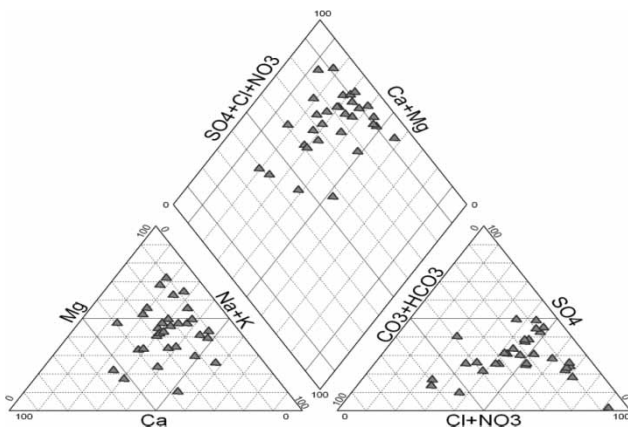
	Minimum	Maximum	Moyenne	Ecart type
pH	7.1	8.8	8.1	0.46
CE ($\mu\text{S}/\text{cm}$)	650	5,150	1,929.4	1,169.66
TDS	468	2,741	1,150.5	567.91
Ca^{2+}	18	230	88.7	54.00
Mg^{2+}	8	189	97.9	49.91
Na^+	38	620	153.8	129.77
K^+	1	66	9.6	12.73
HCO_3^-	73	393	192.6	64.89
CO_3^{2-}	0	60	8.1	13.36
Cl^-	63	1,585	344.6	318.30
SO_4^{2-}	35	818	269.9	195.36
NO_3^-	3.7	82.6	35.3	26.52

Ionic concentrations are given in mg/L.

the means, the order of abundance of cations is mainly $\text{Mg}^{2+} > \text{Na}^+ > \text{Ca}^{2+} > \text{K}^+$ (meq/L) and for anions mainly $\text{Cl}^- > \text{SO}_4^{2-} > \text{HCO}_3^- > \text{NO}_3^- > \text{CO}_3^{2-}$ (meq/L).

Hydrochemical facies

Based on Piper diagram interpretation (Figure 2), various hydrochemical facies were identified, including Mg-Cl, Na-Cl, Ca-Cl, Mg- SO_4 , Na- SO_4 , and under-represented Ca- HCO_3 can be found in this groundwater; however, the majority of samples belong to Mg-Cl (39%) water type followed by Na-Cl (26%) and Mg- SO_4 (19%). The plot of the chemical analyses shows a clear trend against chloride

**Figure 2** | Piper diagram of groundwater samples.

and a tendency to magnesium pole. The Mg-Na-Cl- SO_4 type is a mixture of fresh waters from a dolomitic environment and brackish water distributed in the central and western parts, linked to evaporitic deposits. Seepage from effective rainfall and/or return of irrigation water could complete the main mineralization process (Bekkoussa et al. 2018).

Correlation matrix

The correlation matrix is used to determine the relationship existing between the different variables (Wu et al. 2014; Li et al. 2019). If the correlation coefficient (r^2) is greater than 0.7, two parameters are considered strongly correlated; between 0.5 and 0.7, it indicates a moderate correlation at a significance level $p < 0.05$ (Shyu et al. 2011). The correlation matrix (Table 2) shows high correlation ($r^2 \geq 0.79$) between Na^+ , Ca^{2+} , Mg^{2+} , Cl^- , SO_4^{2-} , and TDS, indicating the significant contribution of these elements to the mineralization of water. High correlations are observed between magnesium and chloride ($r^2 = 0.86$) as well as between magnesium and sulfate ($r^2 = 0.81$). That suggests a part of mineralization may also be linked to the dissolution of MgSO_4 and MgCl_2 . Chloride and sodium with $r^2 = 0.81$ confirm a major source coming from the dissolution of halite. Ca^{2+} and Cl^- show a strong correlation ($r^2 = 0.76$), which can hardly be related to the dissolution of CaCl_2 , and potentially with secondary processes such as the ionic exchange between calcium from clay and available sodium, processes more efficient when mineralization increases in accordance with chloride increases. Ca^{2+} and SO_4^{2-} ($r^2 = 0.89$) can be attributed to the dissolution of sulfate minerals (gypsum) with a possible reverse effect of calcite precipitation process named dedolomitization (Kumar & Singh 2015).

Principal component analysis (PCA)

PCA was used to explain the relationship between numerous variables and establish the factors governing groundwater chemistry in the study area (Figure 3(a) and 3(b)). The first three components extracted have eigenvalues greater than 1, and account for 83.13% of the total variance in the data set (Figure 3(a)). The first principal component (PC1) explains 58.87% of the total variance, with high positive

Table 2 | Correlation matrix for the chemical constituents of groundwater

	Ca ²⁺	Mg ²⁺	Na ⁺	K ⁺	Cl ⁻	SO ₄ ²⁻	CO ₃ ²⁻	HCO ₃ ⁻	NO ₃ ⁻	pH	TDS
Ca ²⁺	1										
Mg ²⁺	0.79	1									
Na ⁺	0.52	0.69	1								
K ⁺	0.62	0.45	0.4	1							
Cl ⁻	0.76	0.76	0.8	0.5	1						
SO ₄ ²⁻	0.89	0.81	0.7	0.3	0.6	1					
CO ₃ ²⁻	0.18	0.21	0.18	0.16	0.15	0.18	1.00				
HCO ₃ ⁻	0.20	0.10	0.12	0.27	0.12	0.03	0.20	1			
NO ₃ ⁻	0.05	0.00	0.01	0.00	0.00	0.02	0.01	0.01	1.00		
pH	0.03	0.08	0.11	0.02	0.10	0.06	0.36	0.00	0.12	1.00	
TDS	0.83	0.94	0.83	0.55	0.94	0.79	0.19	0.15	0.01	0.06	1.00

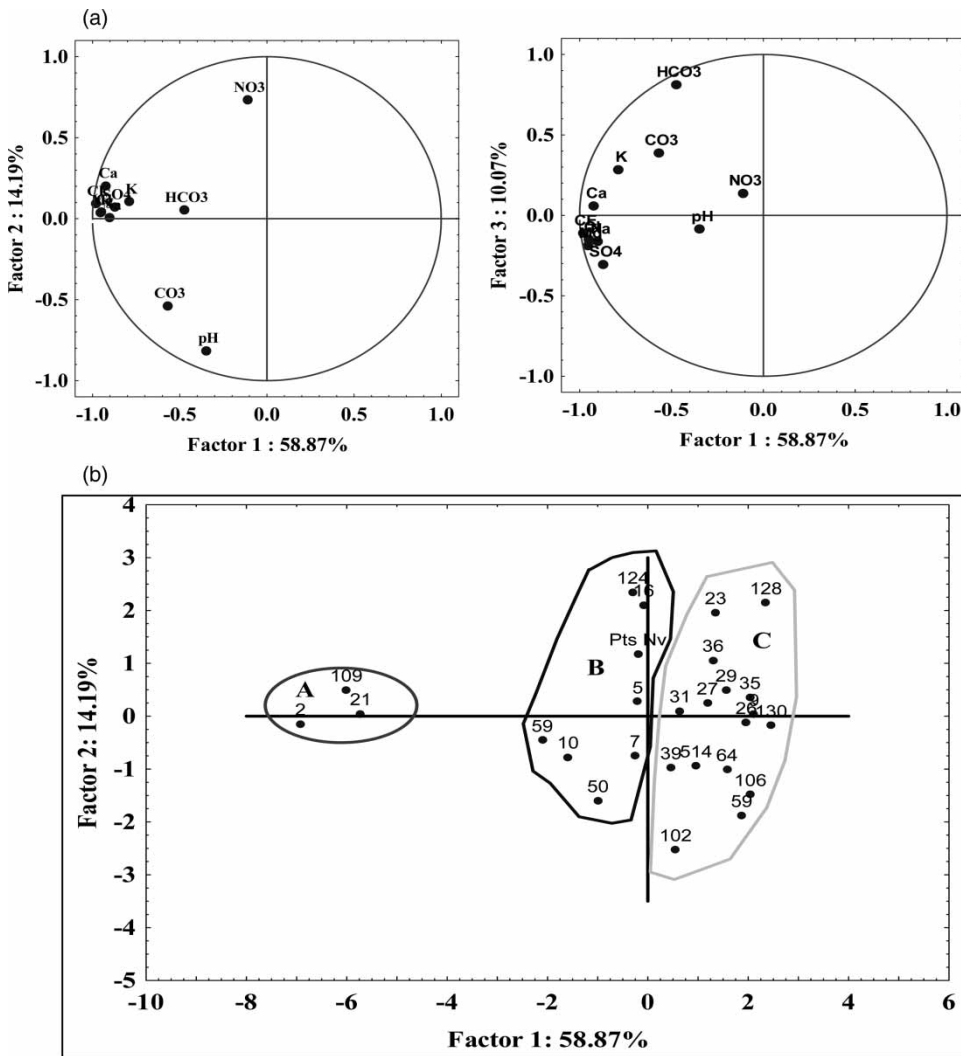


Figure 3 | Results of principal component analysis (PCA). (a) Variables (chemical parameters) graph and (b) individual (observations) graphs.

loading in Ca^{2+} , Mg^{2+} , Na^+ , K^+ , SO_4^{2-} , Cl^- , and EC. This major factor describes the mineralization of groundwater by water–soil/rock interactions. Component 2 explains 14.19% of the total variance and has a strong positive loading on NO_3^- , pH, and CO_3^{2-} . PC2 can be defined as an anthropogenic component due to groundwater contamination by anthropogenic activities, such as urbanization and agricultural activities. Nitrate concentrations in groundwater vary between 3.7 and 82.6 mg/L with a mean value of 35.3 mg/L. Principal component 3 (PC3) explains only 10.07% of the variance. Projection of individuals (sampled wells) on F1–F2 factorial map indicates that F1 axis allows separating weakly and highly mineralized waters (Figure 3(b)).

The more the wells are negative on the F1 axis, the more the water is mineralized. Group A consists of only 11% of the water samples and is characterized by highly mineralized water with an average EC of 2,864.6 $\mu\text{S}/\text{cm}$. Group B includes 37% of water samples and is characterized by moderate mineralization with a mean EC of 1,407 $\mu\text{S}/\text{cm}$. Group C concerns 52% of the water samples, representing the weakly mineralized waters, characterized by an average EC of 856 $\mu\text{S}/\text{cm}$.

Origins of major ions and mineralization processes

Ionic relationships

Major elements vs TDS values show groundwater mineralization is mainly dominated by Mg^{2+} , Na^+ , Ca^{2+} , Cl^- , and SO_4^{2-} contents (Table 2). The Na^+ versus Cl^- plot (Figure 4(a)) shows most samples are plotted along the 1:1 line, suggesting sodium and chloride are derived from dissolution of halite (Li *et al.* 2016a, 2016b). The excess of Cl^- over Na^+ as observed in a few samples could be attributed to the anthropogenic sources such as domestic effluents, septic tanks, and agricultural fertilizers, dissolution of other evaporate minerals (MgCl_2 , CaCl_2) or cation exchange. The plot of $\text{Ca}^{2+} + \text{Mg}^{2+}$ vs Cl^- (Figure 4(b)) shows an increase with respect to Cl^- concentration, showing a significant contribution of these cations to the groundwater salinization, linked to the dissolution of evaporite minerals (MgCl_2 , CaCl_2).

As shown in Figure 4(c), the samples can be grouped into three clusters. The first represents samples plotting near the 1:1 line (gypsum dissolution line). The second is

formed by samples situated below the 1:1 line and may be due to the dissolution of other evaporite minerals such as MgSO_4 . Calcite precipitation would also contribute to lower calcium with higher EC. The third cluster shows an excess of calcium with respect to sulfate as observed, indicating another origin of Ca^{2+} which is possibly the cation exchange process (Li *et al.* 2018), by which the Na^+ is adsorbed by clay minerals on their surface against the release of Ca^{2+} according to the reaction: $(\text{Ca-clay}(s) + 2\text{Na}^+ \rightarrow \text{Na}_2\text{-clay}(s) + \text{Ca}^{2+})$.

To investigate the importance of ion-exchange processes in groundwater chemistry, we have examined the relationship between the concentration of $(\text{Na}^+ + \text{K}^+ - \text{Cl}^-)$ against $(\text{Ca}^{2+} + \text{Mg}^{2+}) - (\text{SO}_4^{2-} + \text{HCO}_3^-)$ (Figure 4(d)). Without the exchange process all data should be close to the origin (McLean *et al.* 2000). The pictorial evidence for cation exchange is given by the linear relationship between $(\text{Ca}^{2+} + \text{Mg}^{2+}) - (\text{SO}_4^{2-} + \text{HCO}_3^-)$ and $(\text{Na}^+ + \text{K}^+ - \text{Cl}^-)$ with the slope equal to -1 (Garcia *et al.* 2001). In our study, water samples conform to the following linear formula:

$$Y = -0.942 X + 1.199 \quad r^2 = 0.965$$

close to the theoretical value of -1 , indicating cation exchange between Na^+ , Ca^{2+} , and Mg^{2+} . However, the difference between the fitted slope and theoretical value also indicates that cation exchange is not the only factor affecting the concentrations of Na^+ , Ca^{2+} , and Mg^{2+} in groundwater, as shown above.

Saturation state

In order to understand the origin and evolution of groundwater mineralization, the SI has been calculated. The results revealed that almost all groundwater samples are oversaturated with respect to calcite ($-0.99 < \text{SI} < 1.78$) and dolomite ($-1.76 < \text{SI} < 3.62$) minerals, suggesting equilibrium or precipitation of these minerals. Geological condition (limestone and evaporites) and hot semi-arid climate induces (hot semi-arid) precipitation–dissolution/dry–wet season cycle in the soil, favoring mineralization of groundwater and increase of the SI leading to precipitation

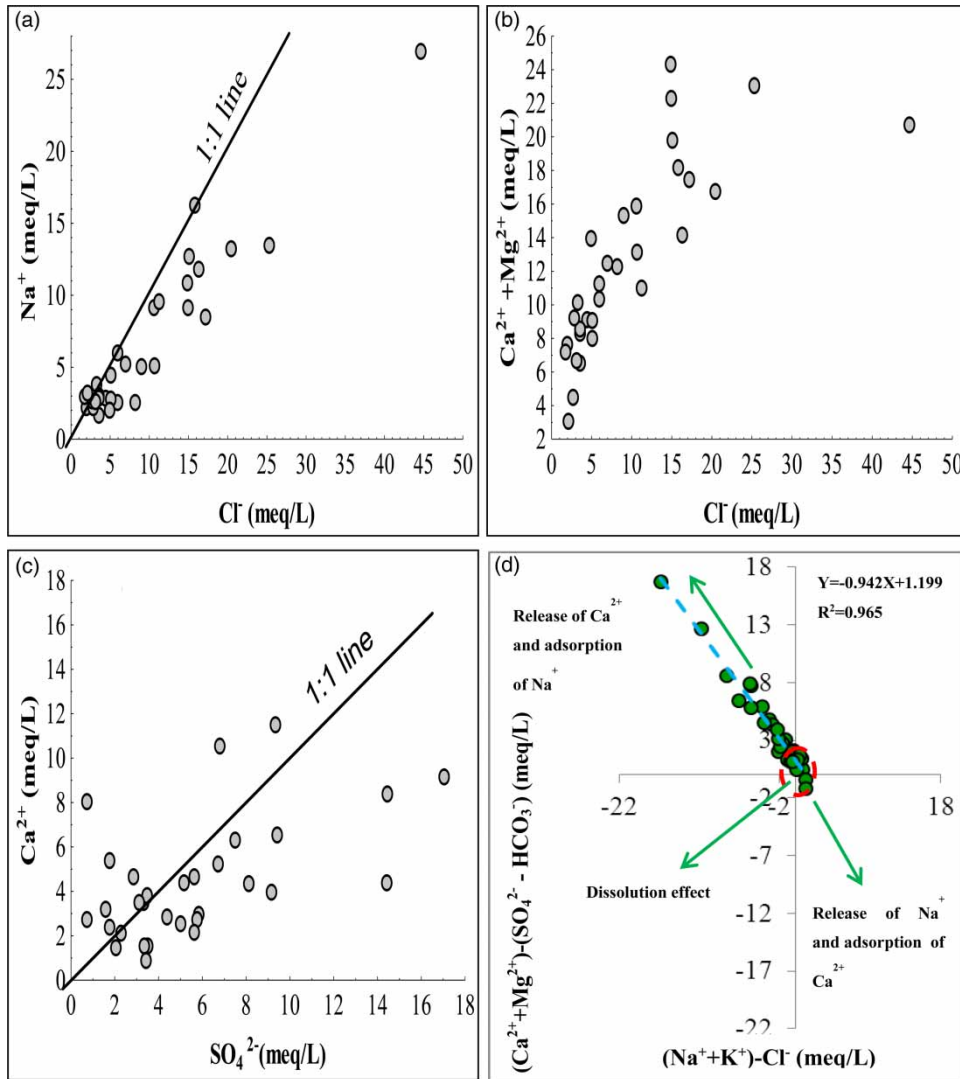


Figure 4 | Relationship between major elements: (a) Na^+/Cl^- , (b) $\text{Ca}^{2+} + \text{Mg}^{2+}/\text{Cl}^-$, (c) $\text{Ca}^{2+}/\text{SO}_4^{2-}$, (d) $[(\text{Ca}^{2+} + \text{Mg}^{2+}) - (\text{HCO}_3^- + \text{SO}_4^{2-})]/(\text{Na}^+ + \text{K}^+) - \text{Cl}^-$.

of calcite and dolomite (Kumar & Singh 2015). Oversaturation of these minerals indicates that water has enough residence time to reach equilibrium. Therefore, the precipitation of these carbonate minerals can potentially decrease and/or stabilize the concentrations of Ca^{2+} , Mg^{2+} , and HCO_3^- along the groundwater flow direction.

Spatial distribution of the physico-chemical parameters

The salinity distribution map (Figure 5(a)) shows lower EC values are located in the south of the study area, in the aquifer recharge zone on the plain borders

(Cretaceous formation of Guelt-stel and Sebaa Rouss). On the other hand, higher conductivity values characterize wells located in the northwestern and central (near Ain Oussera City) zones of the plain. These high conductivity values suggest both natural processes and anthropogenic sources contribute to the geochemistry of groundwater in the plain. The distribution of salinity levels partially conforms to the principal groundwater flow direction and may be controlled by the residence time within the aquifer. Typically, the groundwater salinity will increase with depth and residence times due to chemical interactions with aquifer materials and

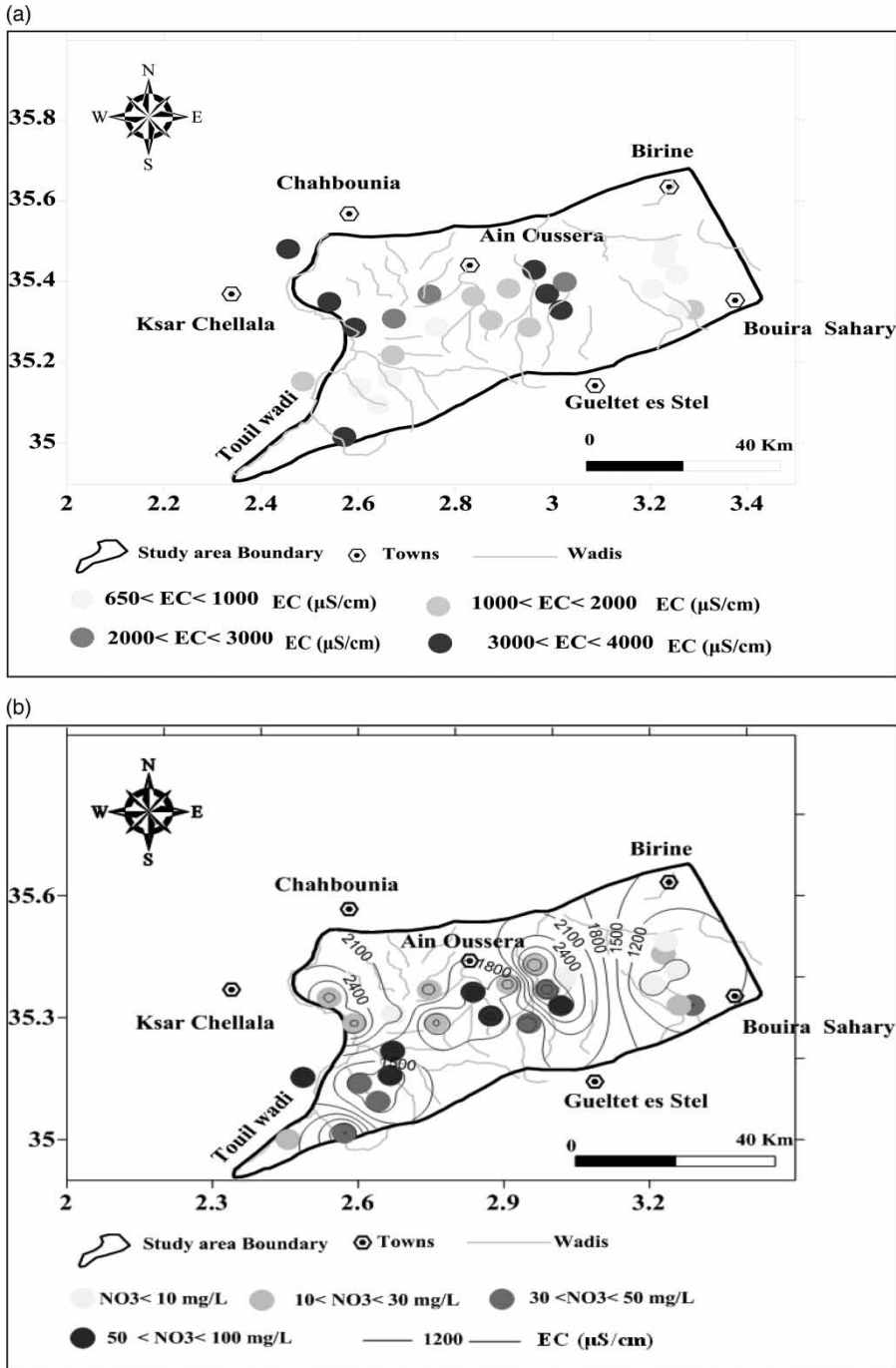


Figure 5 | Spatial distribution map of EC (a) and NO_3^- (b).

possible mixing with older mineralized water along flow paths.

Nitrate (NO_3^-) is a familiar pollutant in groundwater. Nitrate pollution from diffuse agricultural sources is the

main cause of the deterioration of water quality. Large amounts of nitrate in drinking water are a cause of methemoglobinemia (also known as blue baby syndrome), a blood disorder primarily affecting infants under six months

of age (Bengtson & Annadotter 1989). Nitrate concentrations varied from 3.7 to 82.6 mg/L, and about 29% of the samples have nitrate concentrations that exceed the drinking water standards of 50 mg/L (WHO 2006). The spatial distribution of nitrate concentrations (Figure 5(b)) shows that the highest values (up to 50 mg/L) are detected in the southwestern and central zones. The increase of nitrate concentrations is an indication of anthropogenic pollution which is mainly due to high use of fertilizers in the agricultural activities in the plain and to the discharge of domestic untreated wastewater in the urban area (Ain Oussera City). High levels of NO_3^- in groundwater could be reduced by regulating agricultural activities and fertilizer application. Local governments should take action to reduce nitrogen contamination in local groundwater.

CONCLUSION

In the present study, statistical analysis and geochemical methods were applied to investigate the major hydrochemical processes controlling water mineralization in the plain of Ain Oussera. The hydrochemical characteristics of groundwater indicate the order of abundance of the major cations and anions are in the following order: $\text{Mg}^{2+} > \text{Na}^+ > \text{Ca}^{2+} > \text{K}^+$, and $\text{Cl}^- > \text{SO}_4^{2-} > \text{HCO}_3^- > \text{NO}_3^- > \text{CO}_3^{2-}$. The distribution of the groundwater samples in a Piper diagram reveals the majority of samples belong to Mg-Cl water type and are followed by Na-Cl, and Mg- SO_4 . Hydrochemical results demonstrate groundwater mineralization is controlled by natural and anthropogenic processes. Natural processes including water-rock interaction such as the dissolution of evaporates, precipitation of carbonate minerals, and cation exchange reactions are caused by the interaction with clay minerals. Anthropogenic process comprises the contamination from human activities such as sewage effluents and agricultural fertilizers. A PCA was performed on groundwater to identify geochemical processes controlling groundwater geochemistry and to classify the groundwater samples. The first three components of the PCA account for 83.13% of the total variance in the data set.

The integrated approach of statistical and geochemical methods has proved to be potential and effective for investigating the mineralization processes controlling groundwater

chemistry. This work represents a base for future hydrogeological studies that will be helpful for effective water management and sustainable development of groundwater resources in the study area.

REFERENCES

- Bekkoussa, S., Bekkoussa, B., Taupin, J. D., Patris, N. & Meddi, M. 2018 Groundwater hydrochemical characterization and quality assessment in the Ghriss Plain basin, northwest Algeria. *Journal of Water Supply: Research and Technology—AQUA* **67**, 458–466. doi:10.2166/aqua.2018.013.
- Bengtson, G. & Annadotter, H. 1989 Nitrate reduction in a groundwater microcosm determined by 15N gas chromatograph mass spectrometry. *Applied and Environmental Microbiology* **55** (11), 2861–2870.
- Cloutier, V., Lefebvre, R., Therrien, R. & Savard, M. M. 2008 Multivariate statistical analysis of geochemical data as indicative of the hydrogeochemical evolution of groundwater in a sedimentary rock aquifer system. *Journal of Hydrology* **353**, 294–313.
- Domenico, P. A. & Schwartz, F. W. 1998 *Physical and Chemical Hydrogeology*, 2nd edn. John Wiley & Sons, Inc, New York, USA.
- Everitt, B. S. & Hothorn, T. 2011 *An Introduction to Applied Multivariate Analysis with R*. Springer, New York, USA.
- Farnham, I. M., Johannesson, K. H., Singh, A. K., Hodge, V. F. & Stetzenbach, K. J. 2003 Factor analytical approaches for evaluating groundwater trace element chemistry data. *Analytical Chimica Acta* **490**, 123–138.
- Garcia, M. G., Del Hidalgo, M. & Blesa, M. A. 2001 Geochemistry of groundwater in the alluvial plain of Tucuman Province, Argentina. *Hydrogeology Journal* **9**, 597–610.
- Kaiser, H. F. 1958 The varimax criteria for analytical rotation in factor analysis. *Psychometrika* **23**, 187–200.
- Kettab, A., Mitiche, R. & Bennaacar, N. 2008 De l'eau pour un développement durable: enjeux et stratégies. (*Water for a sustainable development: challenges and strategies*). *Revue des Sciences de l'Eau* **212**, 247–256.
- Kumar, A. & Singh, C. K. 2015 Characterization of hydrogeochemical processes and fluoride enrichment in groundwater of South-Western Punjab. *Water Quality, Exposure and Health* **7**, 373–387.
- Li, P., Zhang, Y., Yang, N., Jing, L. & Yu, P. 2016a Major ion chemistry and quality assessment of groundwater in and around a mountainous tourist town of China. *Exposure and Health* **8** (2), 239–252. https://doi.org/10.1007/s12403-016-0198-6.
- Li, P., Wu, J. & Qian, H. 2016b Hydrochemical appraisal of groundwater quality for drinking and irrigation purposes and the major influencing factors: a case study in and around Hua County, China. *Arabian Journal of Geosciences* **9** (1), 15. https://doi.org/10.1007/s12517-015-2059-1.

- Li, P., Tian, R., Xue, C. & Wu, J. 2017 Progress, opportunities and key fields for groundwater quality research under the impacts of human activities in China with a special focus on western China. *Environmental Science and Pollution Research* **24** (15), 13224–13234. <https://doi.org/10.1007/s11356-017-8753-7>.
- Li, P., Wu, J., Tian, R., He, S., He, X., Xue, C. & Zhang, K. 2018 Geochemistry, hydraulic connectivity and quality appraisal of multilayered groundwater in the Hongdunzi coal mine, Northwest China. *Mine Water and the Environment* **37** (2), 222–237. <https://doi.org/10.1007/s10230-017-0507-8>.
- Li, P., Tian, R. & Liu, R. 2019 Solute geochemistry and multivariate analysis of water quality in the Guohua phosphorite mine, Guizhou Province, China. *Exposure and Health* **11** (2), 81–94. <https://doi.org/10.1007/s12403-018-0277-y>.
- Maoui, A., Kherouf, M., Kachi, S. & Nouar, T. 2013 Variographic analysis of chemical and piezometric data from the sandstone aquifer of Ain Oussera, Algeria. *Arabian Journal of Geosciences* **6**, 1307–1324.
- McLean, W., Jankowski, J. & Lavitt, N. 2000 Groundwater quality and sustainability in alluvial aquifer, Australia. In: *Groundwater, Past Achievement and Future Challenges* (O. Sililloo, ed.). Balkema, Rotterdam, The Netherlands.
- Mebrouk, N. 1994 Contribution to hydrogeological study of the Ain Oussera Plain, Algeria. Master's thesis, Oran University (Algeria) (in French).
- Mebrouk, N., Blavoux, B., Issadi, A. & Marc, V. 2007 Geochemical and isotopic characterization of high-Mg groundwater in an endorheic basin, Ain Oussera, Algeria. *Journal of Environmental Hydrology* **15**, 1–20.
- Parkhurst, D. & Appelo, C. 2011 *User's Guide to PHREEQC (Version 2) – A Computer Program for Speciation, Batch-Reaction, One-Dimensional Transport, and In-Verse Geochemical Calculations*. U.S. Department of the Interior/ U.S. Geological Survey, Washington, DC, USA.
- Shyu, G. S., Cheng, B. Y., Chiang, C. T., Yao, P. H. & Chang, T. K. 2011 Applying factor analysis combined with kriging and information entropy theory for mapping and evaluating the stability of groundwater quality variation in Taiwan. *International Journal of Environmental Research and Public Health* **8**, 1084–1109.
- Voutsis, N., Kelepertzis, E., Tziritis, E. & Kelepertzis, A. 2015 Assessing the hydrogeochemistry of groundwaters in ophiolite areas of Euboea Island, Greece, using multivariate statistical methods. *Journal of Geochemical Exploration* **159**, 79–92.
- World Health Organization. 2006 *Guidelines for Drinking Water Quality*, 3rd edn. WHO, Geneva, Switzerland.
- Wu, J., Li, P., Qian, H., Duan, Z. & Zhang, X. 2014 Using correlation and multivariate statistical analysis to identify hydrogeochemical processes affecting the major ion chemistry of waters: case study in Laoheba phosphorite mine in Sichuan, China. *Arabian Journal of Geosciences* **7** (10), 3973–3982. <https://doi.org/10.1007/s12517-013-1057-4>.
- Wu, J., Wang, L., Wang, S., Tian, R., Xue, C., Feng, W. & Li, Y. 2017 Spatiotemporal variation of groundwater quality in an arid area experiencing long-term paper wastewater irrigation, northwest China. *Environmental Earth Sciences* **76** (13), 460. <https://doi.org/10.1007/s12665-017-6787-2>.
- Wu, J., Li, P., Wang, D., Ren, X. & Wei, M. 2019 Statistical and multivariate statistical techniques to trace the sources and affecting factors of groundwater pollution in a rapidly growing city on the Chinese Loess Plateau. *Human and Ecological Risk Assessment*. <https://doi.org/10.1080/10807039.2019.1594156>.
- Zaidi, F. K., Mogren, S., Mukhopadhyay, M. & Ibrahim, E. 2016 Evaluation of groundwater chemistry and its impact on drinking and irrigation water quality in the eastern part of the Central Arabian graben and trough system, Saudi Arabia. *Journal of African Earth Sciences* **120**, 208–219.

First received 4 August 2019; accepted in revised form 22 November 2019. Available online 17 December 2019